



## Investigation of lateral exciton transfer of coexistent quantum dot systems

Jia-Ren Lee, Chien-Rong Lu, and Jen-Yi Jen

Citation: *Journal of Applied Physics* **104**, 073523 (2008); doi: 10.1063/1.2990771

View online: <http://dx.doi.org/10.1063/1.2990771>

View Table of Contents: <http://scitation.aip.org/content/aip/journal/jap/104/7?ver=pdfcov>

Published by the [AIP Publishing](#)

---

### Articles you may be interested in

[Optical characterization of CdSe quantum dots with metal chalcogenide ligands in solutions and solids](#)

*Appl. Phys. Lett.* **99**, 023106 (2011); 10.1063/1.3610456

[Observation of efficient transfer from Mott–Wannier to Frenkel excitons in a hybrid semiconductor quantum dot/polymer composite at room temperature](#)

*Appl. Phys. Lett.* **97**, 263106 (2010); 10.1063/1.3529450

[Lateral redistribution of excitons in CdSe/ZnSe quantum dots](#)

*Appl. Phys. Lett.* **80**, 473 (2002); 10.1063/1.1432743

[Photoluminescence study of CdTe/ZnTe self-assembled quantum dots](#)

*Appl. Phys. Lett.* **74**, 3011 (1999); 10.1063/1.123996

[Zero-dimensional excitonic properties of self-organized quantum dots of CdTe grown by molecular beam epitaxy](#)

*Appl. Phys. Lett.* **73**, 3757 (1998); 10.1063/1.122885

---

A horizontal banner with an orange-to-yellow gradient background. At the top center, the text '2014 Special Topics' is written in a large, white, sans-serif font. Below this text are five circular icons, each containing a different material structure and a label: 1. 'PEROVSKITES' with a red and black lattice structure. 2. '2D MATERIALS' with a blue and red lattice structure. 3. 'MESOPOROUS MATERIALS' with a green and black porous structure. 4. 'BIOMATERIALS/ BIOELECTRONICS' with a yellow and black structure. 5. 'METAL-ORGANIC FRAMEWORK MATERIALS' with a brown and black structure. At the bottom left, the 'AIP | APL Materials' logo is displayed. At the bottom right, a red ribbon contains the text 'Submit Today!' in white.

# Investigation of lateral exciton transfer of coexistent quantum dot systems

Jia-Ren Lee,<sup>1,a)</sup> Chien-Rong Lu,<sup>2</sup> and Jen-Yi Jen<sup>3</sup>

<sup>1</sup>*Department of Physics, National Kaohsiung Normal University, Kaohsiung 824, Taiwan*

<sup>2</sup>*Department of Physics, National Taiwan Normal University, Taipei 116, Taiwan*

<sup>3</sup>*Department of Physics, Tamkang University, Tamsui 251, Taiwan*

(Received 14 June 2008; accepted 14 August 2008; published online 7 October 2008)

The optical characterization of the ZnCdSe/ZnSe quantum dot (QDs) system is studied by photoluminescence (PL) spectrum measured at temperatures from 22 to 300 K. The distinct quenching rates of spectral integrated intensity demonstrate that there are divergent lateral exciton transfer modes between two types of coexistent QDs with different sizes and densities. The smaller and denser QD assemblies are advantageous to trigger lateral migration of thermally activated excitons due to their shallower localization and more coupling channels. However, the carrier repopulation-induced redistribution of excitonic emission energy is contrarily observed in the deepest localized case. The extra redshift of transition energy with increasing temperature is attributed to the incompletely three-dimensional excitonic confinement induced by the morphological features. In contrast with scanning probe techniques, using PL as spectral probe is a nondestructive way to explore inner morphology of capped multiple quantum structure. © 2008 American Institute of Physics. [DOI: 10.1063/1.2990771]

## I. INTRODUCTION

In accordance with the three-dimensional (3D) constraint-induced atomiclike  $\delta$ -function density of states, quantum dots exhibit large oscillator strengths, and consequently high electron-hole recombination efficiency.<sup>1-3</sup> Besides allowing the comprehensive study of physics in a zero-dimensional semiconductor system, these discrete energy levels are expected to produce a number of advantageous properties for optoelectronic device applications.<sup>4-11</sup> Localized excitons of II-VI semiconductors still exist at room temperature, so there is a potential for new devices to utilize their characteristics.<sup>12-16</sup> The studies on II-VI materials have chiefly focused on the CdSe/ZnSe system. However, with a room temperature band gap of 1.67 eV, the CdSe/ZnSe system can only contain the spectral scope from red to green, not the blue and ultraviolet regions.<sup>17-19</sup> As is well known, Zn<sub>1-x</sub>Cd<sub>x</sub>Se can be utilized to spread its spectrum through the whole visible range by modifying the  $x$  value. Therefore, awareness of promising optoelectronic applications based on ZnCdSe makes the investigation of ZnCdSe QDs even more attractive.

In this work, we report the investigation of optical and growth properties of ZnCdSe/ZnSe QD systems epitaxially through the critical thickness by photoluminescence measurements. The divergent temperature evolutions of emission intensity and excitonic transition energy induced by the different morphological features are observed. The characteristics are discussed through the involving lateral exciton transfer mechanism.

## II. EXPERIMENT

The studied low-dimensional quantum heterostructures were grown on the GaAs (001) substrate by hot wall epitaxy. A 50 nm ZnSe buffer layer was first grown on the substrate and followed by three periods of 2.2 nm (sample D) or 9.5 nm (sample S) thick ZnCdSe QD layers with 20 nm ZnSe interbuffer layers, then capped with 50 nm ZnSe. The growth temperature is 235 °C. After deposition of each layer, the growth was interrupted for 20 min; meanwhile, the substrate temperature was decreased to 100 °C for reducing the interdiffusion processes. The concentration of Cd is 33%, as determined by x-ray diffraction. The spectral probe was performed by photoluminescence using 442 nm line of the He-Cd laser as the excitation source. The sample temperature was controlled by a closed-cycle He cryostat system. The spectrally dispersed luminescences were collected from 500  $\mu$ m diameter laser excitation apertures of each sample and detected by a cooled photomultiplier attached to a 1 m double monochromator (Jobin Yvon U1000). The spectral resolution of the spectrometer system is 0.3 meV.

## III. RESULTS AND DISCUSSION

Figure 1 shows the spectral features of samples D and S measured at 50 K, where the spectral intensities are normalized. It is notable that the spectra of thicker sample S dominate by only a single symmetrical line while those of thinner sample D consist of two distinct ones (labeled as A and B). By comparing with the spectral features of ZnCdSe quantum well system,<sup>20,21</sup> we can find that the temperature evolutions of both emission energy and linewidth are consistent with the three lines originating from excitonic transitions of QDs; the details were reported in Ref. 22. The unique reduction in full width at half maximum (FWHM) in QD emission as the temperature increases was attributed to more frequent tunneling process between nearby QDs with predominant sizes.<sup>18</sup>

<sup>a)</sup> Author to whom correspondence should be addressed. Present address: No. 62, Shengzhong Rd., Yanchao Township, Kaohsiung County 824, Taiwan. Electronic mail: kk22cc@nkn.edu.tw. Tel.: 886-919-376720. FAX: 886-7-6051383.

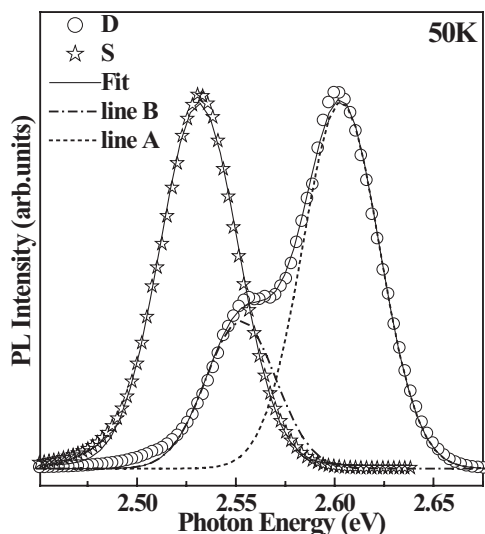


FIG. 1. The spectra of sample of D (circle symbol) and S (star symbol) measured at 50 K; the spectral intensities are normalized. The profiles are fitted by Gaussian lines.

In addition, the lower exciton binding energy of smaller dot is induced by the leakage of the exciton wave function into the surrounding barriers. Therefore, with rising temperature, carriers confined in small dots will be liberated first and may be captured by adjacent larger dots.<sup>23</sup> The two spectral profiles of the thinner ZnCdSe/ZnSe QD system shown in Fig. 1 have different energies and intensities. The higher energy line (line A) with higher intensity is suggested to be originated from smaller and higher density QDs (type A), while the lower energy side (line B) with lower intensity corresponds to larger and lower density QDs (type B). However, the symmetrical single line of the sample S spectra with lowest energy indicates that only one sort of large size QDs exists when epitaxial coverage exceeds 9.5 nm.

In order to verify that the spectral features are indeed QD related, not attributable to wetting layer (WL), the different characteristics between WL and QDs are compared from previous studies.<sup>23–26</sup> In addition to the monotonically increased temperature evolution in FWHM of WL (in contrast with the significant narrowing in FWHM of QDs), the FWHM of WL is also much smaller than that of QDs. The differences of FWHM between QDs and WL are observed to be 30 meV,<sup>25</sup> 55 meV,<sup>23</sup> 75 meV,<sup>24</sup> and 96 meV (Ref. 26) at the lowest temperature. However, the difference of FWHM between lines A and B is merely 3 meV. Therefore, the two bands are both indeed QD-related optical responses. Actually, the two QD emissions of sample D spectra should be attributed to either of the ground state transitions of two types of QDs or the ground and first excited state emissions of a single type of QDs. Nevertheless, the latter possibility can be excluded because the intensity ratio of line A to line B is nearly constant as the excitation power density is increased by 80 times.<sup>22</sup> As previously established,<sup>27</sup> higher excitation power density provides more sufficient photoexcited carriers to fill up the ground state and then more residual carriers will occupy the first excited state to enhance its emission intensity, i.e., higher intensity ratio of line A to line B could be expected as higher power density is provided. Furthermore,

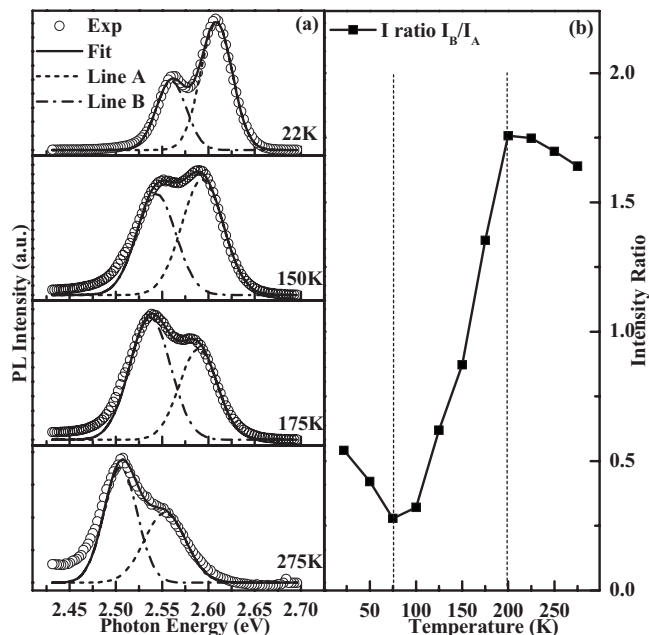


FIG. 2. (a) The spectral intensity and fitting results of sample D measured at different temperatures. (b) The temperature dependence of integrated intensity ratio ( $I_B/I_A$ ) of line B to line A.

the invariable intensity ratios of line A to line B at different excitation power densities correspond with the constant density ratio of type A to type B QDs. Therefore, the two QD emissions can be ascribed to the ground states of two kinds of QDs with distinct size and density by the behavior of both temperature evolution and power dependence of spectral feature.

The different platelet modes between CdTe/ZnTe and CdSe/ZnSe systems have been demonstrated in recent investigations.<sup>28,29</sup> In the CdTe/ZnTe case,<sup>28</sup> the clusters of dots are superimposed on top of a several hundred nanometer-sized two-dimensional (2D) platelet, which provides an efficient channel for coupling between the QDs. Such morphology permits electronic interaction between QDs separated by distances much larger than their size. In the CdSe/ZnSe case,<sup>29</sup> the coexistence of 2D ZnCdSe platelets and 3D islands was verified; the platelets were found to act as precursors for the formation of the 3D islands. The spectral feature of platelets shows a behavior typical of the emission of excitons confined in a quantum well, where the FWHM increases monotonically with temperature. The difference of FWHM between platelets and islands is about 30 meV at the lowest temperature. However, in the  $\text{Zn}_{0.67}\text{Cd}_{0.33}\text{Se}/\text{ZnSe}$  QD system studied here, the monotonic increasing of temperature evolution in FWHM is not observed. Furthermore, the difference of FWHM between lines A and B of sample D is one order smaller than that between platelets and islands at 22 K. Therefore, the two spectral features of sample D both originate from excitonic emission of fully developed QDs. Figure 2(a) shows the spectral profiles and fitting results of sample D at different temperatures. The growth and decline in relative intensities between these two lines are observed with rising temperature. Line A acts as main structure of spectral features at low temperature. At room temperature, line B surpasses line A and contrarily

dominates the spectrum. The phenomenon indicates that line A possesses higher decay rate of intensity with increasing temperature. The temperature evolution of spectral integrated intensity ratio ( $I_B/I_A$ ) of line B to line A is presented in Fig. 2(b). In the range from 75 to 200 K,  $I_B/I_A$  raises rapidly as temperature increases, i.e.,  $I_A$  declines faster than  $I_B$  with ascendant temperature. According to the correspondence between spectral integrated intensity and carrier amount distribution of QDs, the divergent intensity decay rates are attributed to different thermal-redistributed mechanisms of the confined excitons within these two types of QDs, respectively. In dense type A QD case, the lateral transfer processes are significant in the exciton dynamics of such quantum structure due to high coupling between close neighbor QDs. However, inadequate thermal energy at low temperature can only effectuate, through tunnel process, lateral migration of exciton. Therefore, the integrated intensity ratio of these two lines at lowest temperature reliably reflects the density proportion of these two types of QDs. As the raising temperature exceeds critical value, the sufficient thermal energy will enhance the escape and recapture mechanisms of carrier and further provide more efficient lateral transfer modes. Since there are higher quantum confined energies (shallower localization) and more coupling channels owing to the smaller size and more crowded populations of type A QDs, the carriers have more possibilities to get enough thermal activated energy and then depart from their originally occupied QDs. Accordingly, the carrier mobility of denser type A QDs is enhanced to bring on characteristics similar to 2D quantum structure, such as more rapid decay rate of emission intensity. In contrast, the larger and sparser type B QDs are more arduous to perform the lateral transfer processes due to lower quantum confined energy (deeper localization) and longer interval between two dots. Thus more gradual temperature dependence of integrated intensity is observed in type B QDs. In addition, the thermally escaped carriers from type A QDs are possibly trapped by other nonradiative centers or redistributed to empty deeper localized states within type B QDs. Consequently, the different size and density-induced divergent thermally lateral migration mechanisms of these two types of QDs are demonstrated by their diverse temperature evolutions of spectral features from 75 to 200 K. With regard to the more placid temperature trends of intensity ratio observed respectively below 75 K and above 200 K, the deficient thermal energy at lower temperature is difficult to activate the lateral migration processes. On the higher temperature side, unobvious lateral transfer performance is induced by quenching exciton amount within type A QDs, and intense carrier-phonon interactions also weaken integrated intensity of line B.

The descending temperature evolutions of spectral peak energy resulted from the two samples are compared in Fig. 3. In order to suitably display the dissimilar downward trend between the type B QDs grown by  $S$ - $K$  mode within samples D and S, respectively, the downshifted temperature curve of line B peak position is illustrated by dashed line. Comparing with sample D, the epitaxial coverage of sample S is much thicker than the 3D transitional critical thickness of  $Zn_{0.67}Cd_{0.33}Se/ZnSe$  system.<sup>22</sup> Thus QDs of sample S have

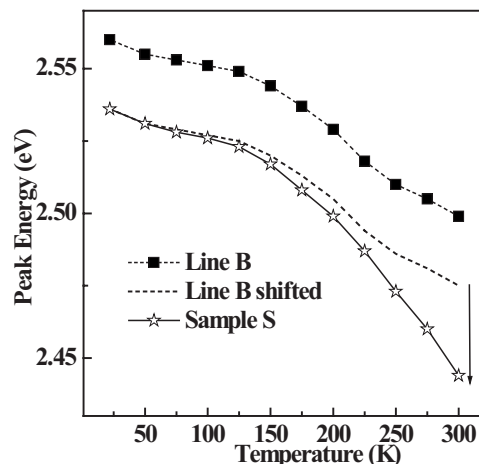


FIG. 3. The temperature evolutions of emission peak energy of line B and sample S. The temperature curve of line B peak position is downshifted and illustrated by dashed line for comparison.

larger size and more amount than those of sample D. This morphological characteristic not only determines the excitonic emission energy and intensity but also affects temperature evolution of spectral peak position. As mentioned above, the spectral intensity decay can be attributed to the carrier escape. However, the enhanced thermally activated migration at high temperature both quenches emission strength by decreasing exciton amount and affects the energy distribution of carriers within assembled QDs. At the lowest temperature, the size distribution of QDs, which are randomly occupied by carriers, mainly determines the energy distribution of carriers and further reflects on spectral profile. The lower energy part of line B is contributed by carriers populated in larger QDs of type B assembly, i.e., the distributive curves of size and energy are mirror reversed. When the temperature exceeds critical value, the threshold thermal energy is capable to activate out the carriers belonging to higher energy part of distribution. Afterward, the higher energy excitons are laterally migrated from their original host QDs to others that own empty levels with steadily lower energy. Therefore, the repopulated excitons reform a new size distribution with smaller size part declining and larger size part growing as contrasted with natural size spread. Furthermore, the resultant peak position of energy distribution of 3D confined carrier shifts to lower energy. The exciton repopulation-induced extra redshift was observed in a four-level QD system.<sup>27</sup> The temperature revolution of excited state in spectral peak position fell more rapidly than that of ground state. In addition, the higher excited state that demonstrated more extra redshift resulted from shallower confinement-induced redistribution of more exciton.<sup>27</sup> However, it is noteworthy that the temperature dependence of peak energy of sample S unexpectedly has faster descending rate than that of line B. As was mentioned above, it would be more difficult for the carriers with deeper 3D confined energy to trigger lateral migration induced by thermal activated process and then gain additional redshift breadth. It means some other involved mechanisms of sample S lead to rapidly downward temperature evolution of emission peak position. One of the possibilities is that denser QDs and more extensive deposited materials

(thicker epitaxial coverage) within sample S are more convenient to perform lateral transfer because of possessing more coupling channels, comparing with those of the isolated type B QDs of sample D. Mackowski *et al.*<sup>24</sup> demonstrated that there are three morphological stages of II–IV QDs with increasing deposition. The third stage is fully developed and isolated QDs. The type B QDs of sample D (2.2 nm) belong to this stage according to the absence of 2D platelet-related optical responses within spectra. Therefore, the excessively deposited sample S (9.5 nm) is expected to have higher density and larger size, i.e., the distance between QDs is shorter. In addition, the redundant epitaxial materials deposited around the dense QDs tend to furnish connecting channels between adjacent QDs. Furthermore, the morphological feature-induced incompletely 3D excitonic confinement of sample S can be regarded as forming a lower effective barrier. Therefore, the additional redshift that resulted from repopulated mechanism with rising temperature is contrarily observed in sample S system, whose excitons possess lower localized energy.

#### IV. CONCLUSION

The thermally redistributive exciton-induced optical characterization of the ZnCdSe/ZnSe coexistent QD system is investigated by PL spectrum measured at temperatures from 22 to 300 K. The analyses of temperature evolutions in spectral integrated intensity and emission energy reveal that the morphological features of QDs serve as an important role in efficiency of lateral carrier migration. The smaller and denser QD assemblies are beneficial to launch lateral transfer of thermally activated excitons due to their shallower localization and more coupling channels. Therefore, the more rapid intensity decay rate of type A QDs contrasting to that of type B assemblies is observed. In addition, since the excitonic transition energy of QDs within sample S is lowest among the three lines, it is expected to be the hardest one to perform lateral transfer mechanism. However, the carrier repopulation-induced redshifted redistribution of excitonic emission energy is contrarily observed in this deepest localized case. The extra redshift of transition energy with rising temperature is attributed to the morphological feature-induced lower effective barrier resulting from the incompletely 3D excitonic confinement.

As established in Ref. 22 etc. and in this paper, the characteristic narrowing of spectral linewidth at critical temperature can be used to verify the 2D to 3D structural transition; the power dependence of integrated intensity can be used to determine the types of QD assemblies; the emission energy can be used to estimate the primary size of QDs; and the temperature evolution of emission intensity and peak position can be used to interpret the lateral exciton transfer processes induced by the morphological characteristics. Consequently, using a well designed PL as a spectral probe can nondestructively provide inner growth properties of capped sample.

#### ACKNOWLEDGMENTS

Financial supports from National Science Council, National Taiwan Normal University, and National Kaohsiung Normal University are gratefully acknowledged.

- <sup>1</sup>M. Grundmann, J. Christen, N. N. Ledentsov, J. Bohrer, D. Bimberg, S. S. Ruvimov, P. Werner, U. Richter, U. Gösele, J. Heydenreich, V. M. Ustinov, A. Yu. Egorov, A. E. Zhukov, P. S. Kop'ev, and Zh. I. Alferov, *Phys. Rev. Lett.* **74**, 4043 (1995).
- <sup>2</sup>J. M. Ulloa, C. Celebi, P. M. Koenraad, A. Simon, E. Gapihan, A. Letoublon, N. Bertru, I. Drouzas, D. J. Mowbray, M. J. Steer, and M. Hopkinson, *J. Appl. Phys.* **101**, 081707 (2007).
- <sup>3</sup>V. Troncale, K. F. Karlsson, D. Y. Oberli, A. Malko, E. Pelucchi, A. Rudra, and E. Kapon, *J. Appl. Phys.* **101**, 081703 (2007).
- <sup>4</sup>M. Fricke, A. Lorke, J. P. Kotthaus, G. Medeiros-Ribeiro, and P. M. Petroff, *Europhys. Lett.* **36**, 197 (1996).
- <sup>5</sup>S. Mackowski, H. E. Jackson, L. M. Smith, J. Kossut, G. Karczewski, and W. Heiss, *Appl. Phys. Lett.* **83**, 3575 (2003).
- <sup>6</sup>S. Mackowski, T. A. Nguyen, H. E. Jackson, L. M. Smith, J. Kossut, and G. Karczewski, *Appl. Phys. Lett.* **83**, 5524 (2003).
- <sup>7</sup>J. Coraux, V. Favre-Nicolin, M. G. Proietti, B. Daudin, and H. Renevier, *Phys. Rev. B* **75**, 235312 (2007).
- <sup>8</sup>S. Mackowski, T. Gurung, T. A. Nguyen, H. E. Jackson, L. M. Smith, G. Karczewski, and J. Kossut, *Appl. Phys. Lett.* **84**, 3337 (2004).
- <sup>9</sup>S. Mackowski, T. Gurung, H. E. Jackson, L. M. Smith, G. Karczewski, and J. Kossut, *Appl. Phys. Lett.* **87**, 072502 (2005).
- <sup>10</sup>C.-H. Chang and Y.-L. Lee, *Appl. Phys. Lett.* **91**, 053503 (2007).
- <sup>11</sup>S. Mackowski, T. Gurung, H. E. Jackson, L. M. Smith, W. Heiss, J. Kossut, and G. Karczewski, *Appl. Phys. Lett.* **86**, 103101 (2005).
- <sup>12</sup>N. T. Pelekanos, J. Ding, M. Hagerott, A. V. Nurmikko, H. Luo, N. Samarth, and J. K. Furdyna, *Phys. Rev. B* **45**, 6037 (1992).
- <sup>13</sup>T. A. Nguyen, S. Mackowski, H. E. Jackson, L. M. Smith, J. Wrobel, K. Fronc, G. Karczewski, J. Kossut, M. Dobrowolska, J. K. Furdyna, and W. Heiss, *Phys. Rev. B* **70**, 125306 (2004).
- <sup>14</sup>S. Mackowski, T. A. Nguyen, T. Gurung, K. Hewaparakrama, H. E. Jackson, L. M. Smith, J. Wrobel, K. Fronc, J. Kossut, and G. Karczewski, *Phys. Rev. B* **70**, 245312 (2004).
- <sup>15</sup>A. Abdi, T. B. Hoang, S. Mackowski, L. M. Smith, H. E. Jackson, J. M. Yarrison-Rice, J. Kossut, and G. Karczewski, *Appl. Phys. Lett.* **87**, 183104 (2005).
- <sup>16</sup>S. Mackowski, H. E. Jackson, L. M. Smith, W. Heiss, J. Kossut, and G. Karczewski, *Appl. Phys. Lett.* **83**, 254 (2003).
- <sup>17</sup>S. Yoon, Y. Moon, T. W. Lee, H. Hwang, E. Yoon, Y. D. Kim, U. H. Lee, D. Lee, H. S. Kim, and J. Y. Lee, *J. Electron. Mater.* **29**, 535 (2000).
- <sup>18</sup>Yu. G. Kusrayev, A. V. Koudinov, B. P. Zakharchenya, S. Lee, J. K. Furdyna, and M. Dobrowolska, *Phys. Rev. B* **72**, 155301 (2005).
- <sup>19</sup>S. Mahapatra, T. Kiessling, E. Margapoti, G. V. Astakhov, W. Ossau, L. Worschech, A. Forchel, and K. Brunner, *Appl. Phys. Lett.* **89**, 043102 (2006).
- <sup>20</sup>Y. Murase, T. Ota, N. Yasui, A. Shikimi, T. Noma, K. Maehashi, and H. Nakashima, *J. Cryst. Growth* **214–215**, 770 (2000).
- <sup>21</sup>D. I. Lubyshev, P. P. Gonzalez-Borrero, E. Marega, E. Petitprez, N. La Scala, and P. Basmaji, *Appl. Phys. Lett.* **68**, 205 (1996).
- <sup>22</sup>J. Y. Jen, C. Y. Lin, J. R. Lee, and C. R. Lu, *J. Phys. Chem. Solids* **69**, 485 (2008).
- <sup>23</sup>G. Karczewski, S. Mackowski, M. Kutrowski, T. Wojtowicz, and J. Kossut, *Appl. Phys. Lett.* **74**, 3011 (1999).
- <sup>24</sup>S. Mackowski, G. Prechtel, W. Heiss, F. V. Kyrychenko, G. Karczewski, and J. Kossut, *Phys. Rev. B* **69**, 205325 (2004).
- <sup>25</sup>M. Larsson, E. S. Moskalenko, L. A. Larsson, P. O. Holz, C. Verdozzi, C.-O. Almbladh, W. V. Schoenfeld, and P. M. Petroff, *Phys. Rev. B* **74**, 245312 (2006).
- <sup>26</sup>C. Jiang and H. Sakaki, *Physica E (Amsterdam)* **26**, 180 (2005).
- <sup>27</sup>J. R. Lee, C. R. Lu, W. I. Lee, and S. C. Lee, *Physica E (Amsterdam)* **25**, 562 (2005).
- <sup>28</sup>T. A. Nguyen, S. Mackowski, T. B. Hoang, H. E. Jackson, L. M. Smith, and G. Karczewski, *Phys. Rev. B* **76**, 245320 (2007).
- <sup>29</sup>C. S. Kim, M. Kim, J. K. Furdyna, M. Dobrowolska, S. Lee, H. Rho, L. M. Smith, H. E. Jackson, E. M. James, Y. Xin, and N. D. Browning, *Phys. Rev. Lett.* **85**, 1124 (2000).